In order to gain objective product, the research shall be supported with series of experiments concerning effects of pressure, high temperatures, time etc. on the presumed designs of composites. The experiments shall be executed i.a. with using a special press and moulds, which allow for manufacturing the fibrous composites featuring multi-layer, cohesive structure and precisely defined, modifiable ballistic properties.

Summary

Completing the project shall allow for delivery of new and innovative solution for manufacturing the ballistic shields. Until now, no composite ballistic shields were offered by domestic manufacturers. The new product will be based on the newest fibrous ballistic materials, which arise in recent years on the worldwide market, and benefit from latest technologies. Developing the product will take execution of multi-directional research, results of which shall allow for optimization models made-up. Reduction of shield's weight and diversification of extra equipment will lead to optimum matching to the needs of the officers of special units subordinated to Ministry of Interior and Administration.

Moreover the commercialization of the research results will happen. The preliminary technical and technological documentation regarding practical applications ready to use/implement will be made. Grant of patent protection is expected for the results of project.

Literature

1. A. Wilczyński; „Polimerowe kompozyty włókniste"; Wydawnictwa Naukowo-Techniczne 1996 Warszawa.
2. W. Jabłoński, J. Wnuk; „Włókno aramidowe bazą produktów innowacyjnych"; BIT; 2000 Bielsko-Biała.
3. W. Błaszczyk, M. Łandwijt; Zeszyty Naukowe Akademii Marynarki Wojennej Rok XLIX Nr 172 K/2; 2008 str. 15.
4. NIJ Standard 0108.01:1985 „Ballistic Resistant Protective Materials".
5. Tencate Advanced Armour Francja, materiały reklamowe; Warunki Techniczne WT-364/ITWW/2003, ITWW „MORATEX", unpublished.
6. http://www.thefind.com/sports/browse-ballistic-shield-level
7. http://www.specops.com.pl/taktyka_czarna/wyposazenie/tarcze_balistyczne/tarcze_balistyczne.htm
8. K. Suddes "The Kent Shield revolutionizes ballistic protection", internet publication (13.02.2007), The One Resource for Police and Law Enforcement (http://www.policeone.com).
9. Warunki Techniczne WT-347/ITWW/2003, ITWW „MORATEX", unpublished.
10. http://www.protechtactical.com/bshields.aspx
11. http://www.global-security-solutions.com/BallisticShield.htm
12. http://www.securityprousa.com/bashleiiiwig.html
13. JEC Composites Magazine, nr 8 str. 26, 2006.
14. „Manual for Dyneema® ballistic panels" – information brochure by DSM.

Computer Simulation of AP Projectile Penetration into RHA

A. Wisniewski, L. Tomaszewski

Military Institute of Armament Technology

1. Introduction

Four stages can be noted in the process of the projectile penetration into armour [1]. In the first stage a wave is created, propagating from the top of the projectile toward its back and generating stresses many times bigger than strength of projectile material, causing plastic strain at its top. The same occurs in the armour, where the stresses cause local transition of armour material in liquid state and, in effect, create a crater.

In the second stage the projectile penetrates into the armour with a constant velocity, and in the third one – the projectile sheds successively the velocity as the result of disappearance of high pressure space. At the last stage a contraction of the crater occurs under the influence of recrystallization and annealing of the armour material.

The above-mentioned process of projectile penetration into armour was analysed with the use of AUTODYN 5 programme. The numerical simulations which were obtained in this way, show changes occurring in the projectile and armour at every moment from the beginning of their contact with the use of discretization, sharing such a complicated effect onto a finite number of simplistic elements. Linear variables of time and space are subjected to discretization. The values of the variables (the displacements, stress, strain, et cetera.) in the function of time, are calculated as a result of the integration of function of entry variables (for example: velocity of projectile) over time, considering values these variables from a previous time step. The discretization of space relies on its division into smaller elements – cells or particles, which interact each other. Then a system of equations is solved, which describes static and dynamic material properties of the projectile and armour. AUTODYN 5 programme contains database of such parameters for different kinds of materials. There exist several methods of computer physics to model phenomena occurring during the collision of the projectile with armour (for example: Lagrange's method, Euler's method, SPH method, etc.).

In AUTODYN 5 programme, the SPH (Smooth Particle Hydrodynamic) method was used, according to it the considered area was covered with particles moving with deforming object. There is calculated sum of interactions for a selected particle of all its adjacent particles. In the every time step of the SPH method, basic stages of calculations are carried out, relying on that, for given initial and boundary conditions, the equations of state, constitutive relations, etc., there are calculated new parameters, such as velocity, stress, force, displacement, etc. in every following cycle and at every point. The main advantage of this method against any other is the lack of mesh on the analysed object. In other methods the mesh covering the examined object can procure significant deformations which sometimes make impossible further calculations. Another advantage of this method is the possibility of the modeling of the cracking effects and the scattering of elements formed from the collision of the projectile and armour.

2. Numerical analysis of projectile penetration into armour

Numerical simulations of the projectile penetration into armour using different dimensions of armour and different physical and mechanical properties of 12.7 mm AP (armour piercing) material were carried out here. In realistic conditions this bullet pierces 20 mm thick steel RHA armour (rolled homogeneous armour) [2]. The goal of computer simulations was to choose optimum parameters of the projectile to obtain the result of projectile penetration into armour closest to reality.

In the all numerical variants RHA steel was used as a homogenous rolled armour which is accessible in the AUTODYN database under the same name. The values of the RHA parameters are shown in Table 1.

In the process of armour penetration the main role is played by the core of the AP projectile, however its remaining elements (coat and pyrotechnical material) have a insignificant influence on the depth of penetration. From this reason only the dimensions and shape of the core of this projectile were considered in subsequent computer simulations.

The material parameters of the projectile were taken from the work [3], where the author explored the capacity of the projectile to pierce ceramic armours. Steel of the 4340 type was used as projectile material with correction of its three parameters. The values of the bulk modulus, specific heat and shear modulus were modified. The 4340a symbol was used for this steel. The parameters of 4340 and 4340a steel were shown in Table 2.

Table 1. The parameters of RHA steel

Steel	RHA	Unit
Equation of state	Shock	
Reference density	7.86	g/cm³
Gruneisen Coefficient	1.67E+00	-
Parameter C1	4.61E+03	m/s
Parameter S1	1.73E+00	-
Parameter Quadratic S2	0.00E+00	s/m
Relative Volume, VE	0.00E+00	-
Relative Volume, VB	0.00E+00	-
Parameter C2	0.00E+00	m/s
Parameter S2	0.00E+00	-
Reference Temperature	0.00E+00	K
Specific Heat	0.00E+00	J/kgK
Strength	von Mises	
Shear Modulus	6.41E+07	kPa
Yield Stress	1.50E+06	kPa
Maximum Expansion	1.00E-01	-
Minimum Density Factor (Euler)	1.00E-04	-
Minimum Density Factor (SPH)	2.00E-01	-
Maximum Density Factor (SPH)	3.00E+00	-
Minimum Soundspeed	1.00E-06	m/s
Maximum Soundspeed	1.01E+20	m/s

Table 2. The parameters of 4340 and 4340a steel

Steel	4340	4340a	Unit
Equation of state	Linear	Linear	
Reference density	7.83	7.83	g/cm³
Bulk Modulus	1.59E+08	**1.30E+08**	kPa
Reference Temperature	3.00E+02	3.00E+02	K
Specific Heat	4.77E+02	**5.00E+02**	J/kgK
Strength	Johnson Cook	Johnson Cook	
Shear Modulus	8.18E+07	**7.20E+07**	kPa
Yield Stress	7.92E+05	7.92E+05	kPa
Hardening Constant	5.10E+05	5.10E+05	kPa
Hardening Exponent	2.60E-01	2.60E-01	-
Strain Rate Constant	1.40E-02	1.40E-02	-
Thermal Softening Exponent	1.03E+00	1.03E+00	-
Melting Temperature	1.79E+03	1.79E+03	K
Strain Rate Correction	1st order	1st order	
Maximum Expansion	1.00E-01	1.00E-01	-
Minimum Density Factor (Euler)	1.00E-04	1.00E-04	-
Minimum Density Factor (SPH)	2.00E-01	2.00E-01	-
Maximum Density Factor (SPH)	3.00E+00	3.00E+00	-
Minimum Soundspeed	1.00E-06	1.00E-06	m/s
Maximum Soundspeed	1.01E+20	1.01E+20	m/s
Maximum Temperature	1.01E+20	1.01E+20	-

The measured velocity of the projectile [3] at the moment of collision with the armour (845 m/s) was taken as the entry variable in numerical simulations.

In the first variant of computer simulation the projectile penetrated armour only 8 mm of depth and the armour bulging was 4.5 mm. For this reason a correction of projectile parameters was necessary.

In the next variant 2 of computer simulations, using 4340 steel parameters, the armour was also not pierced.

In the successive variant 3 the projectile was made from RHA steel. In this case the bulging was the same as in the previous variants, however the depth of penetration increased by about 3% in comparison with the first and second variants. Significant differences in the degree of plastic strain were observed. The decrease of dimension along the axis of projectile in variants 1 and 2 was about 20% higher than in variant 3. The differences in the values of the diameters of so called "projectile mushrooms" were also observed. The projectile mushroom diameter in the variant 3 was about 10% smaller than in variants 1 and 2. The results of simulations for variants 1÷3 are shown in Tables 3 and 4.

Table 3. Results of simulations of penetration of 12.7 mm projectile into RHA layers for variants 1÷3
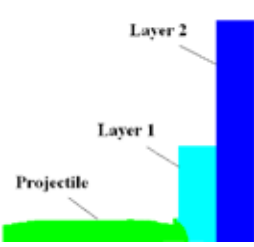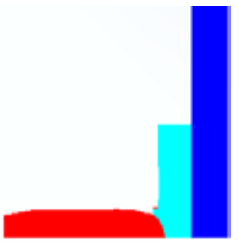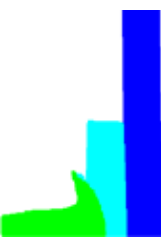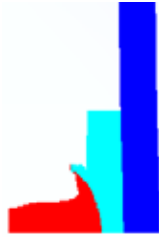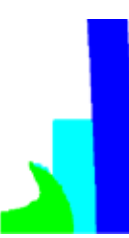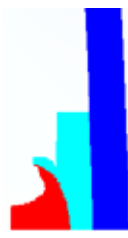
Variant	Material of projectile	Diameter (Ø) and thickness (a) of armour layers, Ø x a, mm	Depth of penetration, DP, mm	Armour bulging d, mm	Final length of projectile, L, mm	Mushroom diameter, D, mm
1	4340a	layer 1: Ø50x10/ layer 2: Ø500x10	8	4.5	18	29
2	4340	layer 1: Ø50x10/ layer 2: Ø500x10	7.9	4.5	18.3	28
3	RHA	layer 1: Ø50x10/ layer 2: Ø500x10	8.2	4.5	22.5	26

In successive calculations the thickness of armour was the same (20 mm), but only one layer of armour was used (Tables 5 and 6).

In regards to the fact that in hitherto simulations the RHA projectile had the best parameters (smaller plastic strain of projectile, bigger depth of armour penetration), the basic (output) projectile material was RHA steel with increased yield stress Re (2500 MPa in variant 4 in relation to 1500 MPa in variant 3). In every next variant, the Re parameter was successively increased (Table 5) to the value of 5000 MPa (variant 7). Results of numerical simulations for variants 4÷7 are shown in Tables 6 and 7.

Table 4. The simulations of penetration of 12.7 mm projectile into RHA layers for variant 1÷3

Variant 1	Variant 2	Variant 3
Projectile: 4340a	Projectile: 4340	Projectile: RHA
Layer 1: Ø50x10; layer 2: Ø500x10		
Cycle 532 Time 0.01 ms	Cycle 537 Time 0.01 ms	Cycle 557 Time 0.01 ms
Cycle 2037 Time 0.04 ms	Cycle 2200 Time 0.04 ms	Cycle 2156 Time 0.04 ms
Cycle 6628 Time 0.14 ms	Cycle 7200 Time 0.14 ms	Cycle 7245 Time 0.14 ms

Variant	Symbol of RHA	Yield stress, R_e, MPa
4	RHAa	2500
5	RHAb	3500
6	RHAc	4500
7	RHAd	5000

Table 5. The yield stress of RHA projectile for variants 4÷7

Table 6. The results of simulations of penetration of 12.7 mm projectile into RHA layers for variants 4÷7

Variant	Material of projectile	Diameter (Ø) and thickness (a) of RHA armour layer 1, Ø x a, mm	Depth of penetration, DP, mm	Armour bulging d, mm	Final lenght of projectile, L, mm	Mushroom diameter, D, mm
4	RHAa	Ø500x20	7.3	3.2	29.6	19
5	RHAb	Ø500x20	11.9	4.9	fragmentation of projectile	16
6	RHAc	Ø500x20	17.3	6.7	fragmentation of projectile	13
7	RHAd	Ø500x20	20.7	9.1	fragmentation of projectile	12.5

Table 7. The simulations of penetration of 12.7 mm projectile into RHA for variants 4÷7

Variant 4	Variant 5	Variant 6	Variant 7
Projectile: RHAa	Projectile: RHAb	Projectile: RHAc	Projectile: RHAd
Cycle 557 Time 0.01 ms	Cycle 557 Time 0.01 ms	Cycle 557 Time 0.01 ms	Cycle 557 Time 0.01 ms
Cycle 2127 Time 0.04 ms	Cycle 2121 Time 0.04 ms	Cycle 2121 Time 0.04 ms	Cycle 2125 Time 0.04 ms
Cycle 4564 Time 0.09 ms	Cycle 4561 Time 0.09 ms	Cycle 4596 Time 0.09 ms	Cycle 4588 Time 0.09 ms

In the Figure 1 armour bulging is shown, as well as the depth of penetration of the armour and the mushroom diameter in function of yield stress for variants 4÷7. Together with the increase of yield stress of the projectile material, its capability of armour penetration also increased. Whereas the mushroom diameter decreases together with the increase of Re. In variant 7 the projectile penetrated 20.7 mm depth of armour, but without piercing it and it was stopped in the armour. The material of the armour underwent large plastic strains, but it retained its cohesion (Table 7). The effect of fragmentation of the projectile into two parts was observed for variants 5÷7.
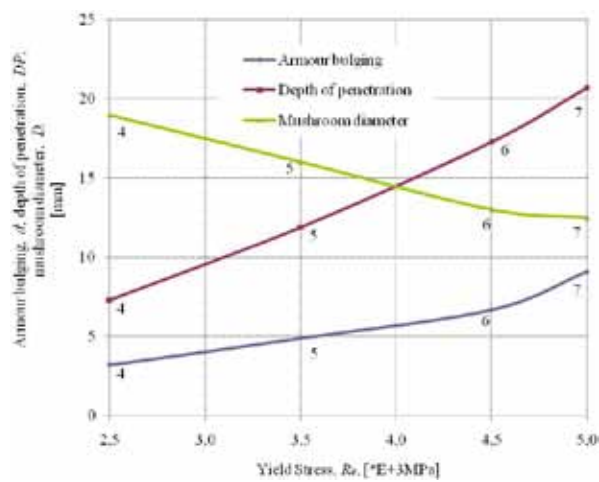

Fig. 1. The changes of armour bulging, the depth of penetration and projectile mushrooming in the function of Re yield stress of projectile material for variant 4÷7

In Figure 2a graphs of projectile velocity along its axis in the function of time for variants 4÷7 are shown. In the 0.02÷0.05 ms time interval, value of the vector of projectile velocity along its axis was the largest during the penetration of armour in variant 4, but at time above 0.05 ms this projectile wasted velocity violently and got stuck in the armour. The projectile in variant 7 kept the value of its velocity above zero for the longest time.

In the Figure 2b graphs of vectors of projectile velocity in orthogonal direction to its axis in the function of time for variants 4÷7 can be observed. The projectile penetrating into armour 4 had the highest velocity. The lowest values of the vectors of projectile velocity were held by the projectile with the highest yield stress (5000 MPa, variant 7).
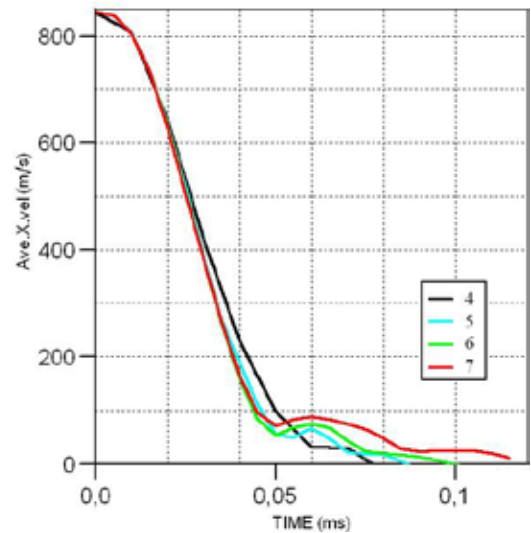
a
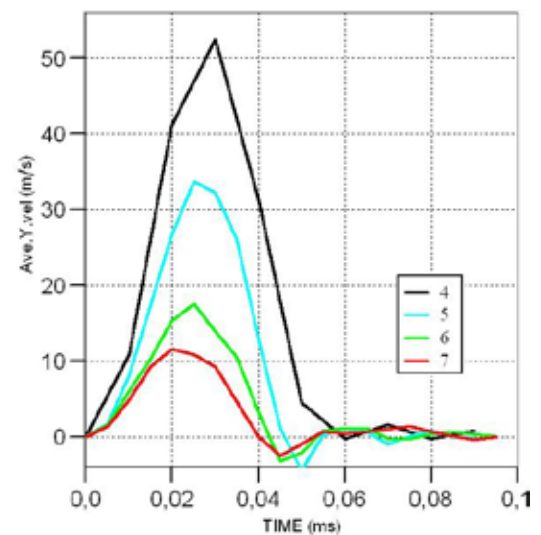
b

Fig. 2. Average velocity of projectile in the function of time for variants 4÷7:
a - along its axis,
b - in orthogonal direction to its axis

In the Figure 3 changes of kinetic energy of the projectile in the function of time are shown. In the 0.02÷0.05 ms time interval, the greatest kinetic energy belonged to the projectile with the smallest yield stress (variant 4). This is related to the greatest strains of the projectile in this variant. At the moment of collision of the projectile and armour the top of the projectile brakes violently, and rear fragments of it move with a velocity similar to its initial value (845 m/s), as a result of plastic strains of the projectile material. The greater these strains are, the lower the yield stress of the projectile material is.

There is also an effect of the projectile mushrooming at the beginning of the penetration

process of the armour in variant 4. The lowest yield stress (1500 MPa) and, connected to it, the most substantial ductility, caused a dissipation of projectile elements in an orthogonal direction to its axis of penetration. This is disadvantageous effect because of the fact that its big portion of kinetic energy is dissipated not along axis of armour penetration, but in a transverse way. In variant 4 at the time above 0.05 ms a sudden drop of the projectile's kinetic energy followed as a result of its velocity drop (Fig. 2a and 2b).
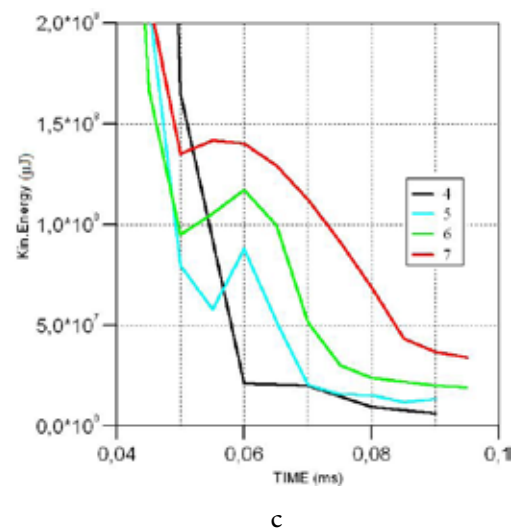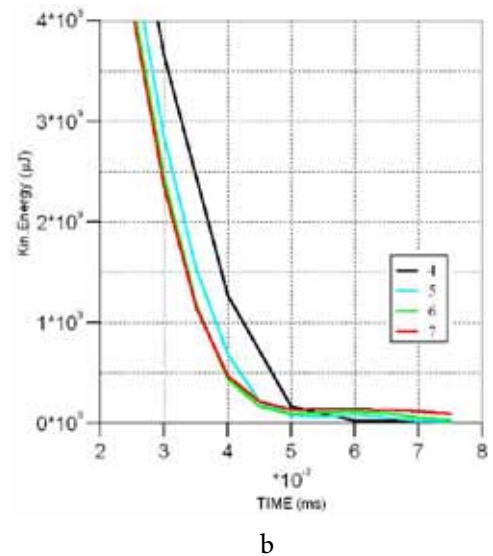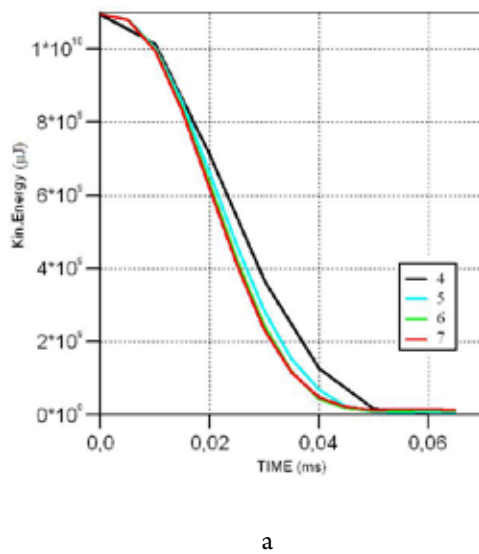

a

b

c

Fig. 3. *The kinetic energy of projectilein the function of several interval times for variants 4÷7:*
a - 0÷0.06 ms,
b - 0.2÷0.08 ms,
c - 0.04÷0.1 ms

3. Conclusions

On the base of above simulations the following conclusions can be presented:

1. The value of time t at which a projectile is stopped in armour rises together with the yield stress of the projectile material (the time of penetration was 60% longer in case of using projectile made from steel with two times higher yield stress).
2. At the initial phase of projectile penetration into armour (0÷0.04 ms) kinetic energy of the projectile is inversely proportional to the yield stress of its material. Above 0.06 ms the higher kinetic energy of projectile is, the higher the yield stress of its material is (Table 8).
3. The lower yield stress of projectile material is, the shorter time of losing kinetic energy during penetrating of RHA armour is (Table 8):

*   in the 0.03÷0.06 ms time interval, the projectile in variant 4 (Re =2500 MPa) lost 99% of its kinetic energy in comparison with 94% of kinetic energy loss for projectile in variant 7 (Re =5000 MPa).
*   in the 0.06 ms time, the projectile in variant 4 had only 14% value of kinetic energy of the projectile in variant

Table 8. Kinetic energy of projectile in its successive stages of penetration process into RHA for variants 4÷7

Variant	Yield stress, R_e, MPa	Kinetic energy of projectile, E_{kin}, for time, t		Decrease of energy, ΔE_{kin}, % $t = 0.03 \div 0.06$ ms	Kinetic energy relations between respective variants 4÷7, %	
		0.03 ms	0.06 ms		$t = 0.03$ ms	$t = 0.06$ ms
4	2500	3.7E9 μJ	2.0E7 μJ	99	$E_{kin4} / E_{kin4} = 100$	$E_{kin4} / E_{kin7} = 14$
5	3500	2.9E9 μJ	8.0E7 μJ	97	$E_{kin5} / E_{kin4} = 78$	$E_{kin5} / E_{kin7} = 57$
6	4500	2.4E9 μJ	1.2E8 μJ	95	$E_{kin6} / E_{kin4} = 65$	$E_{kin6} / E_{kin7} = 86$
7	5000	2.2E9 μJ	1.4E8 μJ	94	$E_{kin7} / E_{kin4} = 60$	$E_{kin7} / E_{kin7} = 100$

Table 9. The influence of the yield stress of projectile material on its plastic strains
and on capability of armour penetration in initial phase (t=0.04 ms) of penetration

Variant	Yield stress, R_e, MPa	Depth of penetration, DP, mm	Length of the rest of projectile, L, mm	Mushroom diameter, D, mm
4	2500	5.7	31.7	19
5	3500	9.3	37.1	15.6
6	4500	13.8	43.1	13
7	5000	15.7	45.6	12.5

4. Projectile made from material with lower yield stress (Re =2500 MPa, on the assumption Ekin=100%) causes the following (Table 9):
- the highest kinetic energy of projectile (in the 0÷0.04 ms time interval) is used mainly for plastic strains of projectile;
- armour penetration is less deeply in the axis of the projectile because it undergoes more plastic strains.

5. Two times higher yield stress of projectile material, i.e. Re =5000 MPa - variant 7 in comparison with projectile material, i.e. Re =2500 MPa - variant 4 causes (in the 0÷0.04 ms time interval) that (Table 9):
- the mushroom diameter is 35% smaller,
- the depth of penetration is 2.75 times bigger.
- the length of the rest of projectile is 43.8% bigger.

6. In variant 3 greater depth of penetration (DP=8.2 mm) and more substantial armour bulging (d=4.5 mm) was obtained than in variant 4 (one-layered armour - DP=7.3 mm, d=3.2 mm) despite the fact that the projectile material in variant 4 had a higher yield stress (2500 MPa in variant 4 in the comparison to 1500 MPa in variant 3). The resulting conclusion is that the protection capability of one-layered steel armours is higher than two-layered steel armours made from the same material.

Literature

1. *Magier M.: Methods to estimate the armour penetration depth by kinetic projectiles. Problemy Techniki Uzbrojenia i Radiolokacji (Problems of Armament Technology and Radiolocation), Wojskowy Instytut Techniczny Uzbrojenia (Military Institute of Armament Technology), Zielonka, 103, 2007.*

2. *Wiśniewski A.: Pancerze - budowa, projektowanie i badanie (Armours - construction, designing and testing). Wydawnictwa Naukowo Techniczne (Scientific-Technology Publisher), Warsaw, 2001.*

3. *Łukasik W.: Protection capabilities of large-sized corundum ceramics. Doctor's thesis. Akademia Górniczo-Hutnicza (Coal-Metallurgy University), Cracow, 2005.*